Structural analysis of Sho-Vel-Tum using balanced cross sections

Molly Carpenter[1] and Bryan Tapp[2]

[1]Department of Geosciences, The University of Tulsa, 800 S. Tucker Drive, Tulsa, Oklahoma 74104. Current address: Chesapeake Energy Company, Oklahoma City, Oklahoma 73118. molly.carpenter@chk.com.

[2]Department of Geosciences, The University of Tulsa, 800 S. Tucker Drive, Tulsa, Oklahoma 74104. jbt@utulsa.edu. Corresponding author.

ABSTRACT

A subsurface study in the Ardmore Basin compares the structural styles of Sho-Vel-Tum with those of the adjoining Arbuckle Uplift in south-central Oklahoma using a simple three-point-problem approach to develop dip-vector maps, strike-line maps and ultimately detailed structure contour maps. Five balanced cross sections were developed using standard techniques. The balanced cross sections provide robust constraints for reconstructing the evolution of the Arbuckle Mountains during the Pennsylvanian.

Sho-Vel-Tum experienced flexural-slip folding and into-the-hinge thrust faulting during transpression. Accommodation space decreases to the northwest along anticlinal hinges. Folding mechanisms, fault trends, and deformation styles suggest that Sho-Vel-Tum and the Arbuckle Uplift are similar.

These methods and ideas used are simple yet innovative in interpreting structurally complex areas in the subsurface. This project shows that the development of strike and dip data can lead to data-driven, well-constrained, and complete balanced cross sections that can guide structural interpretations in the subsurface.

INTRODUCTION

The region in and around Sho-Vel-Tum is known for its structural complexity and has been the subject of debate as to whether the uplift resulted from compression (Taff, 1904; Dott, 1933; Brown, 1984; Naruk, 1994), strike-slip (Ham, 1951; Tanner, 1963; Carter, 1979; Tomlinson and McBee, 1987) and/or transpression through inversion (Granath, 1989; Ferebee, 1991; Tapp, 1995). Southern Oklahoma is the location of a triple junction rift that resulted in a northwest-southeast-oriented aulacogen forming the Arbuckle and Wichita Mountains (Hoffman et al., 1974; Feinstein, 1981). Later deformation of the region occurred during the Pennsylvanian when North America collided with Llanoria (South America and Africa) causing uplift (Houseknecht, 1983). Difficulties arise when interpreting the complex structures in the region due to uncertain geometries of the initial rift-bounding faults and due to the uneven collision between North America and Llanoria. By determining a connection between the Arbuckle Uplift and Sho-Vel-Tum, interpretations can be drawn about the structural styles of the area.

Sho-Vel-Tum is immediately west of the Arbuckle Mountains (Figure 1). This work tested the idea that the trend of increasing deformation seen in the Arbuckle Uplift continued into the subsurface into the Tatums, Sholem Alechem (shortened to Sholem), and Velma Fields that make up part of Sho-Vel-Tum. The project was approached as if it were a field mapping exercise, within the subsurface. Over 300 well logs were studied and over 500 strike and dip values were calculated using the classic three-point-problem construct. The strike and dip values were used to create a series of dip-vector maps throughout Sho-Vel-Tum. Five balanced cross sections were constructed extending from the western Arbuckle Mountains to the southwest into the Sho-Vel-Tum Complex. Stereonets and strain ellipses were also constructed for further structural analysis of each field. The development of strike and dip data lead to data-driven, constrained, and complete balanced cross sections, independent of any initial model bias. The area was treated as a new field area so that the strike and dip data, balanced cross sections, stereonets, and strain ellipses can help guide further structural interpretations of the region.

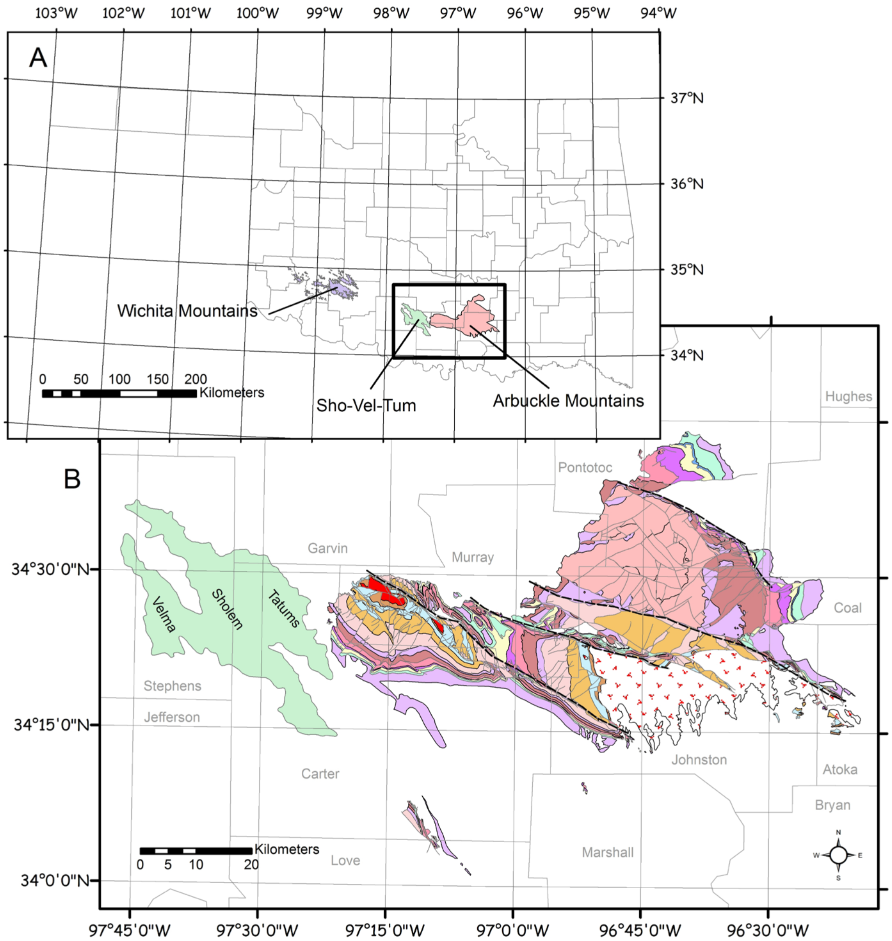

Figure 1. A: Oklahoma map showing the location of Sho-Vel-Tum in relation to the Arbuckle and Wichita Mountains. B: Surface geology of the Arbuckle Mountains showing Pre-Pennsylvanian formations. Major bounding faults are represented by bold dashed lines in the Arbuckle Mountains. Sho-Vel-Tum is shown with the Tatums, Sholem, and Velma Fields labeled. Digital data from Cederstrand (1996), Boyd (2002).

Previous Work

Fields within the Sho-Vel-Tum Complex have been described as compressional or transpressional (Hoard, 1956; Billingsley, 1956; Rutledge, 1956; Granath, 1989; Harmon and Tapp, 2001; Decker, 2002). Hoard (1956) described the Tussy Sector of the Tatums Field as a series of faulted noses, faulted anticlines, and truncated structures. The northwest-oriented anticline in the Sholem Field has been described as compressional (Billingsley, 1956). Steeper dips on the northeast side of this anticline prompted Billingsley (1956) to suggest compression came from the southwest. The apex of this anticline shifts to the southwest with depth (Billingsley, 1965). Both Hoard and Billingsley used well log and drilling data prior to the mid-1950's to describe the structures in the Tatums and Sholem Fields.

The Velma Field is more complex than the Tatums and Sholem Fields and was first studied in the 1950's by Rutledge (1956), who noted that there were two periods of intense folding in the Velma Field, the first in post-Morrowan and the second in post-Hoxbar, and that each of these events was followed by deep erosion. In his interpreted cross section, Rutledge (1956) shows four vertical faults and two anticlinal folds with the axis of the major fold migrating westward with depth and the eastern edge acting as a horst. Rutledge's main data source was drilling information and well logs. Decker (2002) describes the structures in the Velma and Milroy Fields as disharmonic with three levels of structuring. He illustrates the first level as having basement elements that protrude northeast from under the Wichita Uplift causing faulting in the basement rocks and Arbuckle Group. His second level of morphology includes backthrusting in the Arbuckle Group, as well as rabbit-ear folds in the Simpson Group. Detachments in the Caney and Goddard Formations represent the third level of structuring (Decker, 2002). Decker (2002) recognized that folds tighten to the northwest and backthrusting is more prominent towards the northwest as well. Decker (2002) concluded that fold geometries in these two fields do not represent significant strike-slip displacements. Concurrent with Decker, Harmon and Tapp (2001) constructed balanced cross sections in the Milroy Field and conclude that a backthrust model fits the style of deformation along the Velma-Milroy trend. Using seismic data, Jacobson (1984) interpreted a cross section that begins 9.6 km (6 mi) southwest of Velma on the Wichita Uplift and extends northeast through the West Velma Field and ends 4.8 km (3 mi) northwest of the Sholem Field. His cross sections show two major high angle reverse faults protruding from depths below 2,743 m (9,000 ft). The angles on these reverse faults shallow with depth. The northern fault in his cross section, termed the Velma Fault, was interpreted by Perry (1988) as a listric thrust fault with late Virgilian dip-slip displacements of more than 2,896 m (1.8

mi).

Rutledge (1956) believed that the major structures within Velma began to develop with the Wichita orogeny during the late Morrowan period with over 914 m (3,000 ft) of uplift and 610 m (2,000 ft) of Springer removed by erosion (Rutledge, 1956). However, Jacobson (1984) and Perry (1988) concluded that Velma was uplifted 1,524 m (5,000 ft) during the Atokan or very early Desmoinesian, followed by an additional 457 m (1,500 ft) of uplift in the later part of the Desmoinesian.

Granath (1989) used the kinematic relationships between faults systems to predict the horizontal component of slip from incremental strain data in a regional study of the Ardmore Basin. He suggested that the Ardmore Basin was divided into rhombohedral blocks by left-lateral strike-slip followed by transpression in the Late Pennsylvanian (Granath, 1989). This resulted in localized deformation styles connected through fault systems, similar to what was described by Ferebee (1991). Ferebee (1991) suggested that localized compression and extension stresses were transferred vertically and horizontally through faults with slip occurring along discontinuous planes creating sinistral transpressive and transtensional features. Granath's (1989) study described the Healdton Field deformation as dominantly strike-slip; the Kirby Fault as mainly a dip-slip fault with a small right-lateral component; the northern fault in the Velma Field as a high-angle reverse fault; and both the Washita Valley Fault and Criner Hills Uplift displacement as oblique through pure left-lateral strike-slip and pure reverse slip (Figure 2). In his interpretation, the reverse faults in the Velma Field make up a system of faults that eventually connect to the Criner Uplift in the southeast and to the Meers/Washita Valley Fault system in the northwest.

This study was undertaken to examine the structural style of Sho-Vel-Tum in detail to test the models that have been proposed for the areas and to determine if modern balancing methods could be used to develop geometrically and structurally reasonable cross sections in this complex system.

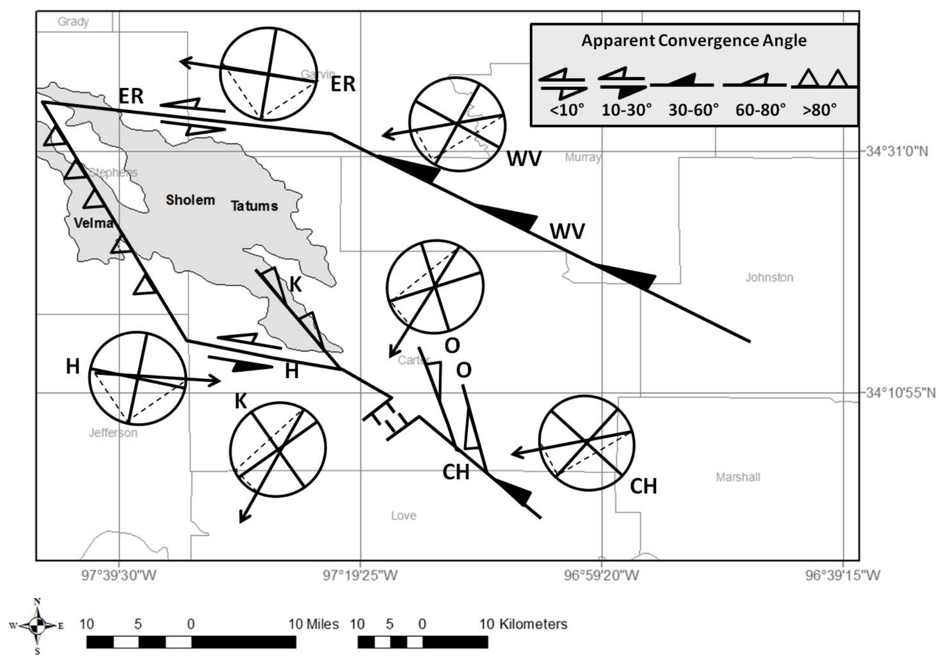

Figure 2. Type and convergence angle for major faults in the Ardmore Basin. Letters represent the fault or field; CH, Criner Hill; O, Overbrook; K, Kirby; H, Healdton; ER, Eola Robertson; and WV, Washita Valley. The circle denotes the fault orientation by the letter, dashed lines represent the strain ellipse axes, and vector represents the displacement convergence to fault normal. Modified after Granath (1989)

Methods

Initial data for the project included basic information and well logs for all of the wells in Stephens and Carter Counties, Oklahoma. Pennsylvanian and older tops were interpreted and correlated for more than 300 of the deeper wells within the Tatums, Sholem, and Velma Fields. Sho-Vel-Tum is the largest oil and gas complex in Oklahoma encompassing over 650 sq km (241 sq mi). More than 21,000 wells have been drilled since 1914 with production occurring in Permian through Ordovician units. The history of exploration throughout Sho-Vel-Tum resulted in a substantial amount of well data for the project.

Three proprietary seismic lines within Sho-Vel-Tum were used to help guide interpretation. The seismic lines are oriented northeast southwest and extend 3 to 6 km (2 to 4 mi) southeast of the Tatums, Sholem, and Velma Fields (Figure 3). When studying the seismic lines, notes were taken and detailed drawings were constructed so that the structures observed could be correlated to other aspects in the project.

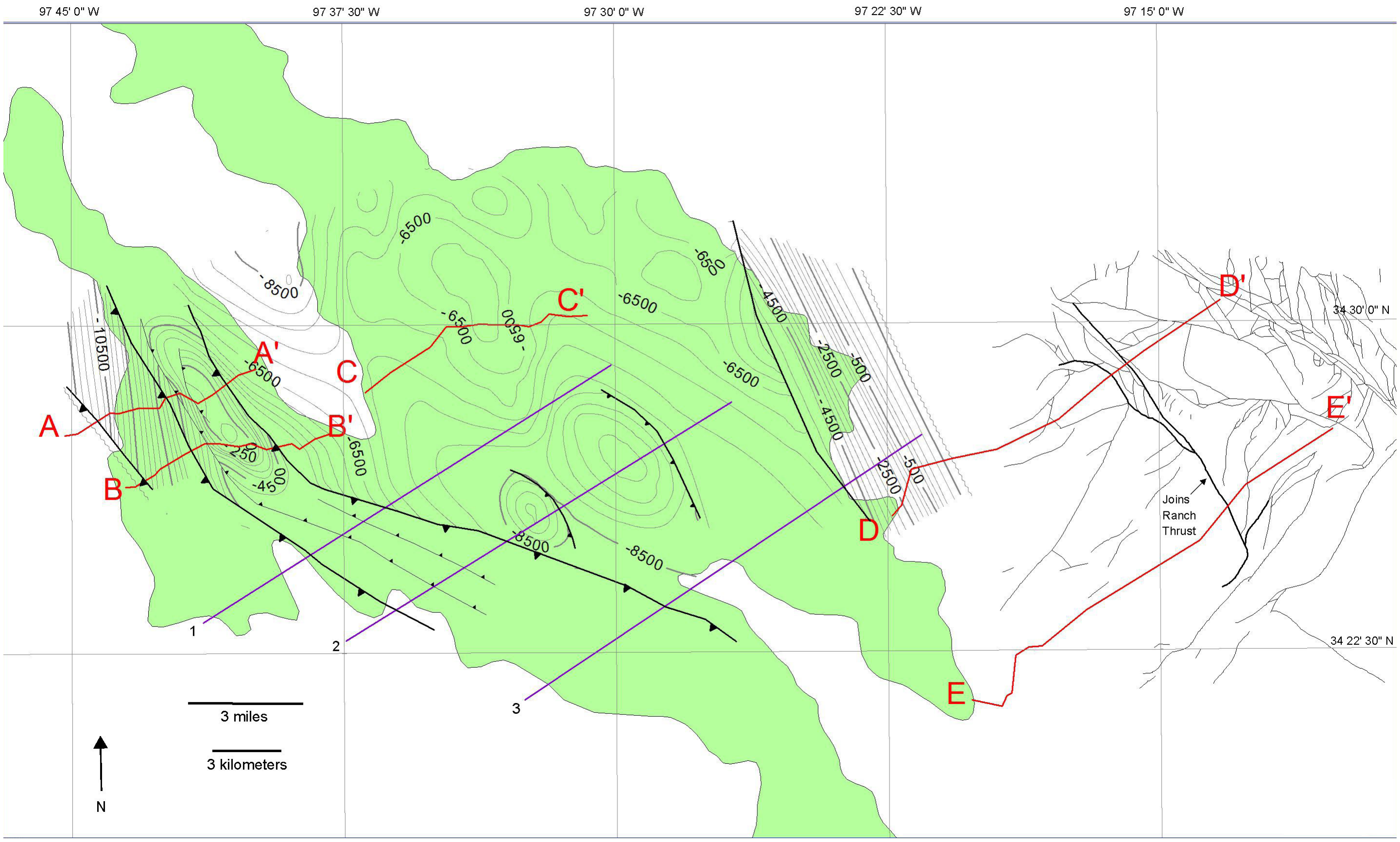

Figure 3. Cross section locations are shown through Sho-Vel-Tum and western Arbuckle Mountains. Surface faults in the Arbuckle Mountains are outlined with the Joins Fault in bold. Contours are on the Sycamore Formation with a 122-m (400-ft) interval. Approximate location of seismic lines 1, 2, and 3 are also shown.

Dip-vector maps were constructed using the interpreted tops from well logs in the Tatums, Sholem, and Velma Fields. Each dip value was calculated through triangulation of three wells on the same top (classic three-point problem). From the three wells, strike lines were drawn and a dip value was calculated using the equation:

$$\text{Dip} = \text{Arctangent}\,[\text{rise/run}] \quad (1)$$

Rise is the change in elevation and run is the horizontal distance between two strike lines. The distance between three wells ranged from 152 m (500 ft) up to 1,520 m (5,000 ft). Overall, 32 dip-vector maps were constructed throughout Sho-Vel-Tum on eight Pennsylvanian to Ordovician formation tops.

A dip value was also calculated using the apparent thickness in well-log signatures and a regional thickness determined from researched values. The calculated dip values were compared to the dip values determined from 3-point problems to verify the dip-vector maps.

Structure maps were developed using all available data: dip-vector maps, strike-line maps, dipmeter data, log tops, and fault geometries from seismic data. Tops were identified in all available logs that penetrated the Mississippian Sycamore Formation or deeper within the Tatums, Sholem, and Velma Fields. Faults were recognized by repeat or missing sections in well logs, however, faults could also be recognized when the contours did not correspond to the dip-vector maps. Fault localities can also be verified using apparent thickness relations in well logs. Discordance between hand contours and dip-vector maps helped to identify fault trends in the structure maps. The fault trends in the structures maps correlated to the faults trends observed in the seismic data. Therefore, the geometry of faults in the seismic data likely represents the geometry of faults in the structure maps. The detailed mapping techniques utilized in developing structure maps allowed for a better understanding of the behavior of faults and folds within Sho-Vel-Tum.

Five cross sections were constructed perpendicular to strike. The cross sections extend over key areas of interest in Sho-Vel-Tum based on the structure maps (Figure 3). Two cross sections extend over the western edge of the Arbuckle Mountains into the Tatums Field, one cross section extends over the Sholem Field, and two cross sections extend over the Velma Field. The locations of the cross sections were chosen using three criteria: the deepest wells, wells with significant features such as faults, and shallower wells for an even spacing between deeper wells. Using these criteria to select cross section wells resulted in significant and complete cross sections perpendicular to strike.

Surface geology over the western Arbuckle Mountains was incorporated in the Tatums Field cross sections and includes outcrop formations, strike and dip data, and surface faults. The surface geology was derived from the map, "Geologic Map and Sections of the Arbuckle Mountains, Oklahoma" (Johnson, 1990). The fault of focus in the western Arbuckle Mountains was the Joins Fault and is the only surface fault included in the cross sections. By tying the cross sections back to the Arbuckle Uplift, the connection between the structural style of the uplift and Sho-Vel-Tum could be analyzed.

When constructing and interpreting each cross section, a dip value was calculated for each formation interval in the well-log signatures. The calculated dip values were then corroborated using the dip-vector maps and dipmeter data when available. The dip data and structure maps helped to locate faults, and by integrating the seismic information, the geometry of the faults could be interpreted. After the cross sections were constructed, they were balanced to test the validity of the interpretation and to test if each was retro-deformable.

Each cross section was balanced by hand through successive attempts to minimize error. If a cross section can be balanced, it is considered retro-deformable, thus verifying the initial interpretation as geometrically reasonable. Both the kinked-bed and line-length methods were used for balancing. In a cross section, the bed layers are straightened and the curvature of bedding is kinked, making the cross section geometrically more accurate for balancing (Mount et al., 1990). This method assumes the thickness is uniform and that a fold hinge occurs at the same point through the bed layers (Mitra, 1992). When balancing a cross section using the line-length method, a pin-line is placed vertically through an area with little deformation (Groshong, 2006). The cross section is balanced from the pin-line by "stretching" each bed layer horizontally from the pin-line. This is done by measuring the length of each bed layer and marking fault contacts. Each measured line length is drawn horizontally from the pin-line with fault geometries drawn at the marked contacts. A cross section is considered balanced when the ends of each bed layer line up vertically and fault geometries are structurally feasible. The amount of shortening is calculated by dividing the total length of the deformed cross section by the total length of the balanced cross section. The percent of error is calculated off the deviance of the longest measured line length and must be less than five percent to be considered balanced (Mitra, 1992). This was accomplished by dividing the shortest measured line length by the longest measured line length. Once a cross section is balanced with less than a five percent error using these methods, then the initial deformed cross section is an acceptable geometric interpretation.

Six Mississippian and older units were kinked and balanced in the five cross sections. The tops of the Sycamore Formation, Hunton Group, Viola Formation, Bromide Formation, Oil Creek Formation, and the Joins Formation were selected because of their relatively equal spacing and definitive log character. Dashed lines represent interpolated layers where erosion has occurred in the cross sections. All of the work was done by hand and then drawn into Corel Draw to generate the final cross section. For each deformed cross section, the balanced section is shown below at a smaller scale in the figures. No vertical exaggeration is used in the cross sections. A scale is shown for both the deformed and balanced section. Formation tops and fault contacts are marked on each well in the cross sections. These marked tops also include younger formations and unconformities that were not balanced. These general attributes were used for the construction of each cross section through Sho-Vel-Tum.

Cross sections D-D' and E-E' extend over the western Arbuckle Mountains into the Tatums Field. Surface geology including strike and dip values were used to construct these cross sections along with well logs from the Tatums Field. Three wells were used to construct cross section D-D' and six wells were used to construct cross section E-E'. The Cool Creek Formation, Butterfly Dolomite, and Timbered Hills Group were included in cross sections D-D' and E-E' because they encompass structural features that are exposed at the surface.

Cross section C-C' extends over the Sholem Field. Fifteen wells were used to construct this cross section with six wells penetrating Mississippian and older strata. Only Mississippian and older units were kinked while the younger formations were kept smooth. This cross section was not balanced due to the lack of significant faults and structures.

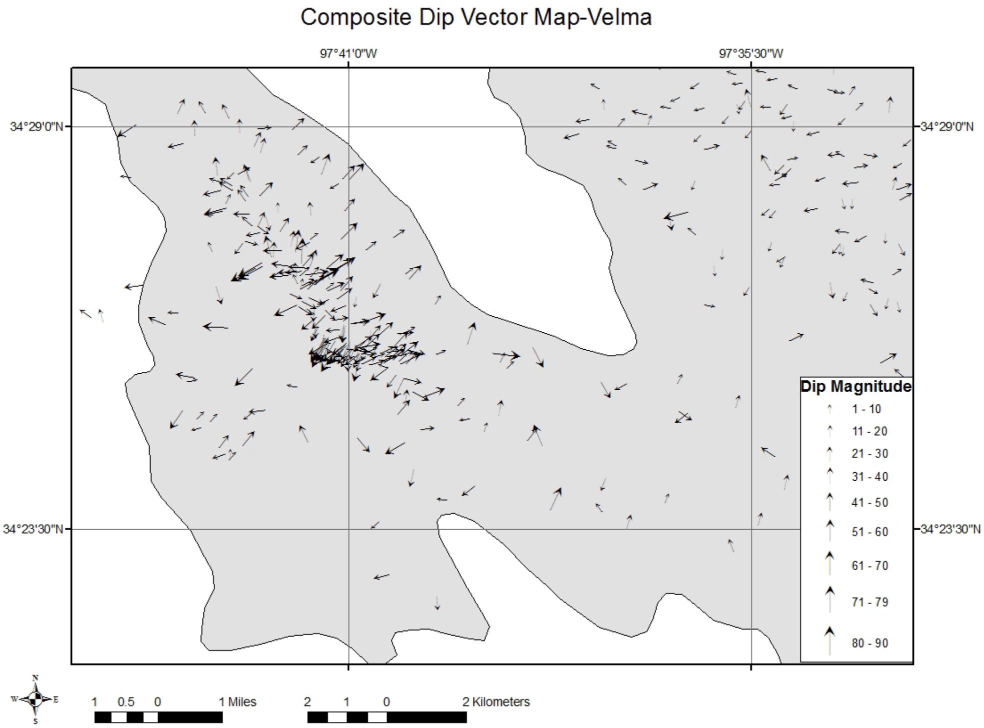

Figure 4. Composite dip-vector map for the Velma Field based on three-point problem solutions for Deese through Viola. Dip directions are shown; longer vectors represent greater dip values.

Results

The dip-vector maps indicate areas of high structural variation, including major faulting and folding within each field. The dip-vector maps for the Tatums Field show random vectors with primarily low dips. Few noticeably higher dips occur along the northeast edge of the Tatums Field where the Arbuckle Uplift begins in the subsurface. These dips represent high deformation along the southwest edge of the Arbuckle Uplift that transforms into low deformation along the northeast edge of Sho-Vel-Tum revealing a separation between the two systems. The Sholem Field also displays very low dip values suggesting that deformation intensity is not continuous from the Arbuckle Uplift. To the southwest, however, there is a dramatic change in the behavior of the dip vectors in the Velma Field. The vectors display dominant trends representing steeply dipping layers and well-defined structures. The geometrical trends of the dip vectors in the Velma Field (Figure 4) reveal a northwest-southeast elongated anticline. The dip-vector trends illustrate that deformation is much less in the Tatums and Sholem Fields than in the Velma Field, suggesting deformation increases to the southwest in Sho-Vel-Tum, but is not a continuation of the Arbuckle Uplift (Simpson-Carpenter, 2011).

In cross section A-A' through the Velma Field (Figure 5), four major reverse faults were mapped including three backthrust faults. The backthrust faults were recognized by three repetitions of the Viola and Joins Formations in a single well. These backthrust faults extend toward the southwest off the first major bounding reverse fault to the northeast in the Velma Field. The first major bounding fault (fault 4) and the series of backthrust faults (fault 3) are interpreted as into-the-hinge thrust faults that occur from room accommodation problems in flexural-slip folding. As shortening increases in a region, the bounding faults absorb the compressional energy creating upwards displacements versus a continuous horizontal deformation pattern. This resulted in a major faulted anticline oriented northwest-southeast creating the dominant structure in the Vel-

Cross sections A-A' and B-B' extend over the Velma Field. The fault geometries mapped through this field were correlated from the trends observed in the seismic lines using dip-vector maps and dipmeter data. Fourteen wells were used to construct cross section A-A' with eight wells penetrating Mississippian or older strata. Sixteen wells were used to construct cross section B-B' with seven wells penetrating Mississippian or older strata. Cross sections A-A' and B-B' are the farthest to the southwest in Sho-Vel-Tum and required detailed mapping efforts due to complex structural features.

Fold and strain analyses were performed to help constrain the structural style of each of each field. Pole data were plotted on the Schmidt Equal Area Net using strike and dip values generated from the three-point problems and analyzed using standard methods. The approximate strain ellipse was calculated from the cross sections to demonstrate the amount of shortening that has occurred through each field. The ellipse was calculated using the greatest amount of shortening for each cross section and was rotated along strike when plotted on a map. The stereonets and strain ellipses gave a further analysis on the style of folding that occurred in each field during deformation.

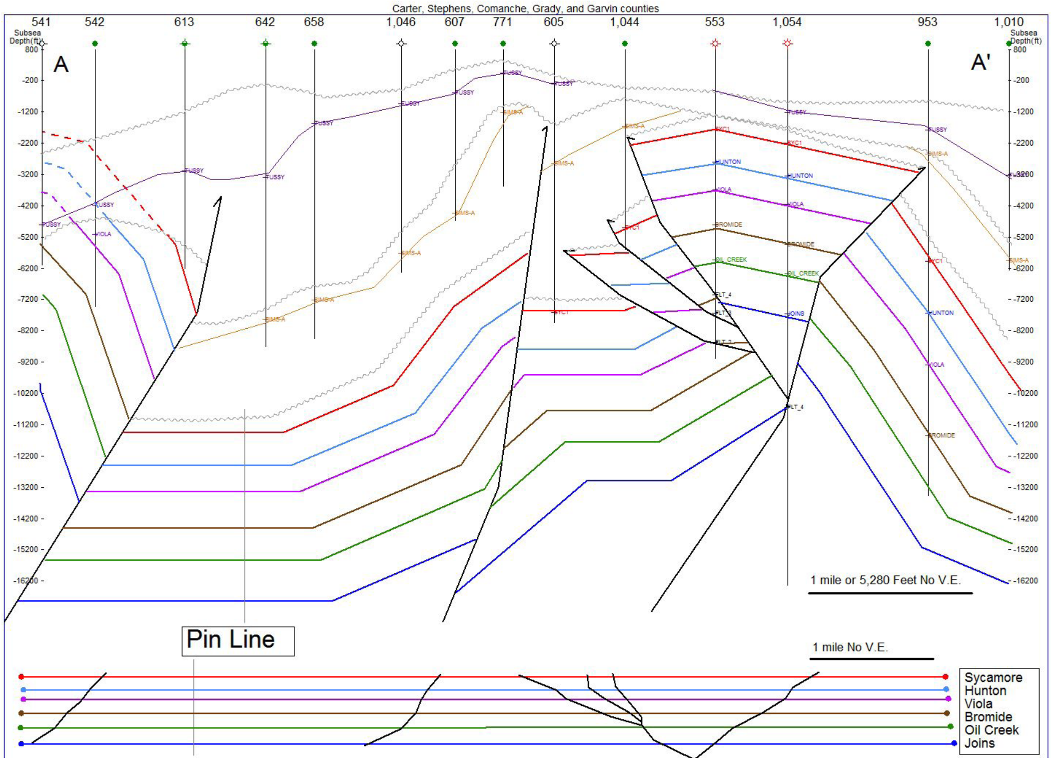

Figure 5. Cross section A-A' through the Velma Field. The well number is shown above the well symbol and can be found in the appendix. Dashed lines represent interpolated layers where erosion has occurred. In cross section A-A' three reverse faults and a series of backthrust faults are mapped. The balanced section is shown with the pin line. A scale is shown for both the deformed and the balanced section.

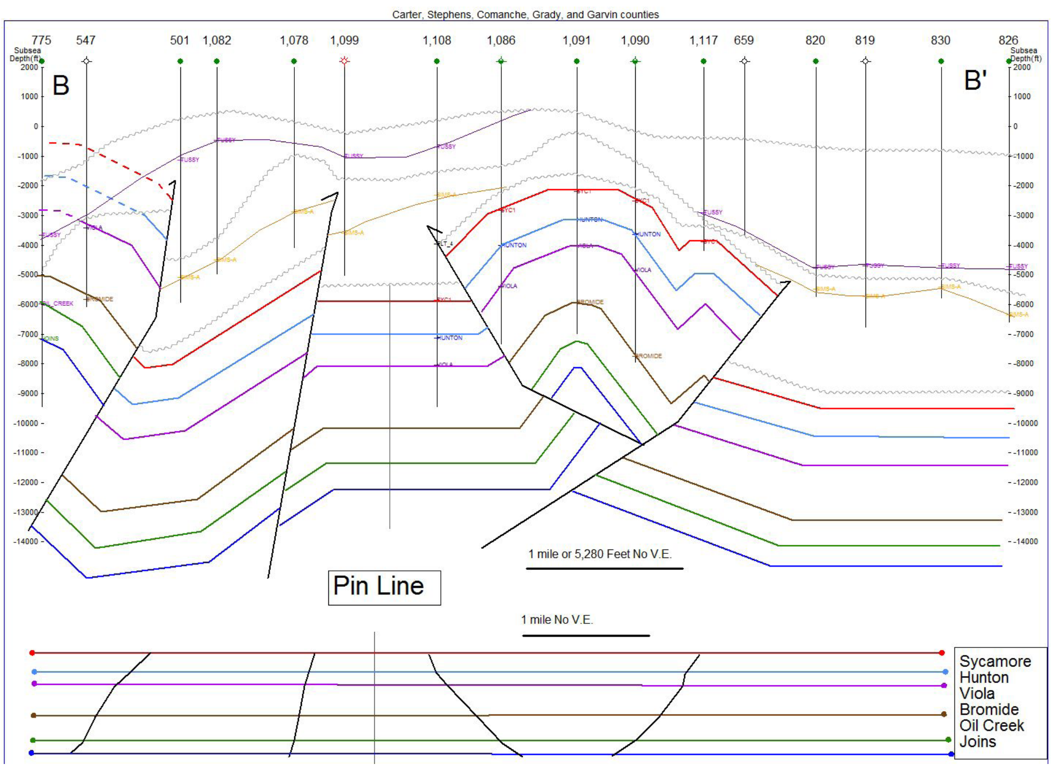

Figure 6. Cross section B-B' through the Velma Field. The well number is shown above the well symbol and can be found in the appendix. Dashed lines represent interpolated layers where erosion has occurred. In cross section A-A' three reverse faults and a series of backthrust faults are mapped. The balanced section is shown with the pin line. A scale is shown for both the deformed and the balanced section.

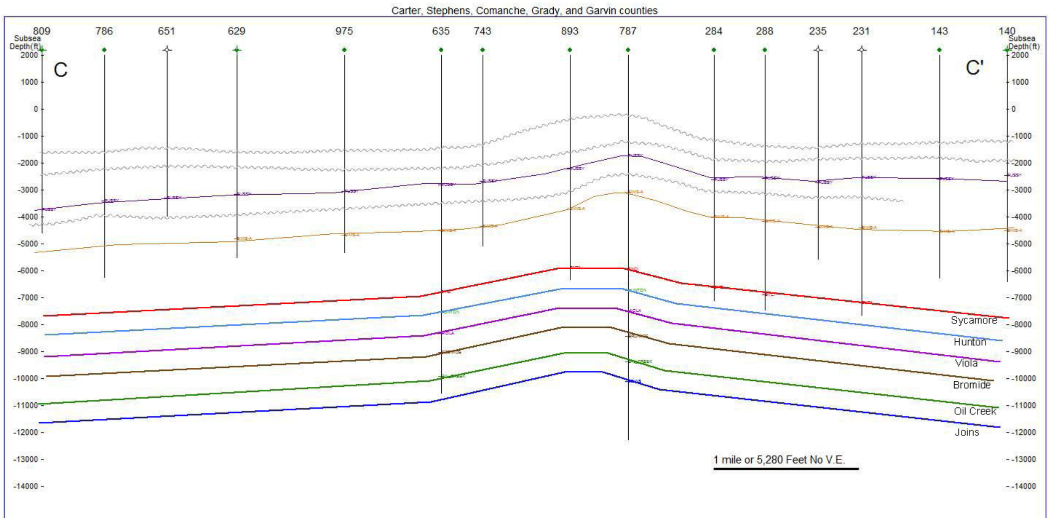

Figure 7. Cross section C-C' through the Sholem Field. A broad gentle anticline is the dominant structure with a slightly steeper dip angle along the northeast limb. The anticline trends northwest southeast. This section was not balanced due to the low levels of shortening.

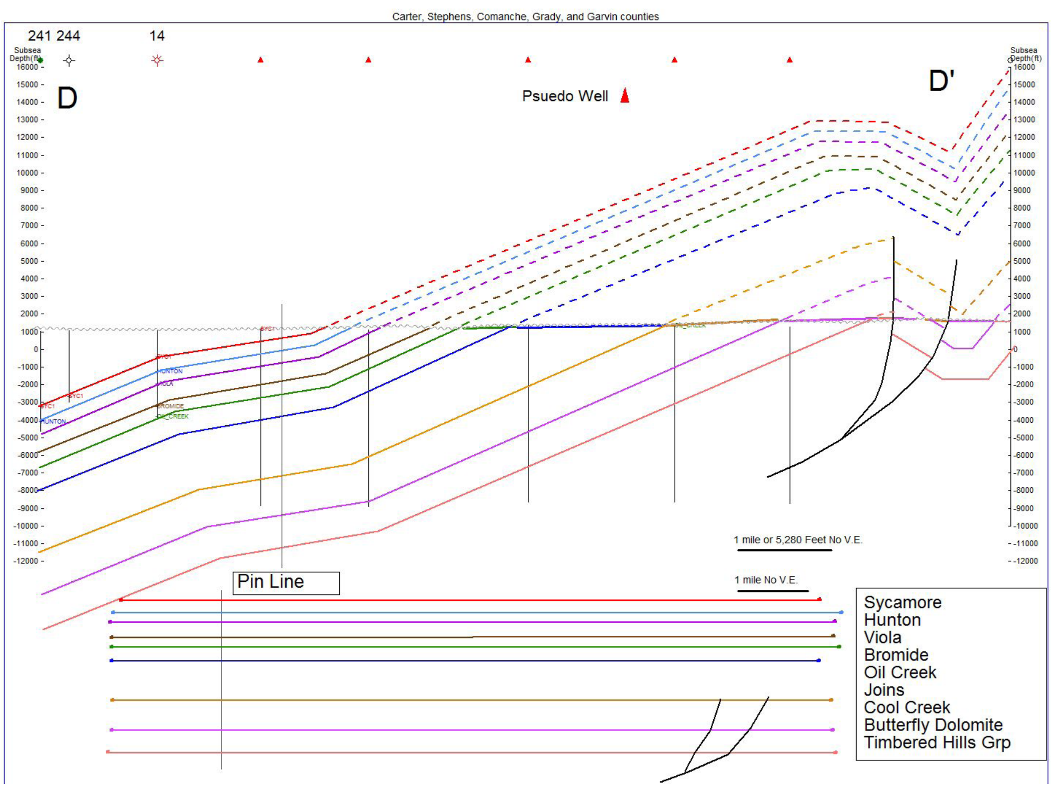

Figure 8. Cross section D-D' through the Tatums Field. The wells used are shown by the number above the well symbol, and can be found in the appendix. Dashed lines represent interpolated layers where erosion has occurred. Pseudo wells do not actually exist. These are vertical profiles at a point that are based on outcrop width and dip in field data. The Joins Faults is split into two segments in D-D'. The balanced section is shown below with the pin line. A scale is shown for both the deformed and the balanced section.

ma Field. The offset for the major bounding fault in cross section A-A' is 396 m (1,300 ft). The offset for each back-thrust fault in cross section A-A' from northeast to southwest is 741 m (2,431 ft), 241 m (790 ft), and 818 m (2,683 ft). Two other high-angle reverse faults were mapped from shallower structures that mimic the offset of the deeper reverse faults. The fault farthest to the southwest (fault 1) is very close to the Wichita Uplift in the subsurface and has a displacement of approximately 1,370 m (4,500 ft) in cross section A-A'. The second fault (fault 2) has an approximate offset of 550 m (1,800 ft) and occurs between fault 1 and fault 4. These two faults strike northwest-southeast and dip to the southwest. Overall, three high-angle reverse faults and three backthrust faults were mapped with a 1.3 % error for cross section A-A' which is 31% shortened.

Four faults intersect cross section B-B' (Figure 6) and can be correlated with the faults in cross section A-A'. The first major reverse fault to the northeast (fault 4) correlates to the bounding fault in cross section A-A'. However, only a single backthrust fault (fault 3) extends off of this fault in cross section B-B'. Cross section B-B' is 25% shortened and multiple backthrust faults may not have developed due to a lesser amount of shortening than in cross section A-A'. The offset for the major bounding fault (fault 4) on cross section B-B' is 1,036 m (3,400 ft) and the offset for the backthrust fault (fault 3) is 518 m (1,700 ft). The fault farthest to the southwest in cross section B-B' can be correlated to fault 1 in cross section A-A' and has an offset of 1,585 m (5,200 ft). A second reverse fault can be correlated to fault 2 in cross section A-A' and has an offset of 300 m (1,000 ft). The error for balanced cross section B-B' is 1.8%. Cross sections A-A' and B-B' were developed using well-log data, dip-vector maps, apparent-thickness relations, and structure maps. The mapped faults have structurally reasonable geometry and offset and balance with less than 2% error.

A single cross section extends through the Sholem Field. This cross section, C-C' (Figure 7), displays a gentle anticline oriented northwest-southeast. The dips along this anticline are slightly steeper along the northeast limb. The lack of major structures in the Sholem Field suggests that Sho-Vel-Tum is disconnected from Arbuckle deformation.

In the cross sections through the Tatums Field, the Joins Fault cuts through the hinge of a fold up on the Arbuckle Uplift while a major fault in northeast Tatums Field separates the Arbuckle Uplift from Sho-Vel-Tum. On cross section D-D' (Figure 8) the Joins Fault has an offset of 366 m (1,200 ft), but on cross section E-E' (Figure 9) it has an offset of 122 m (400 ft). The amount of shortening in cross section D-D' is 10% and the amount of shortening in cross section E-E' is 7%. The Joins Fault acts as a transpressional into-the-hinge thrust fault with less accommodation room towards the northwest. A major fault separat-

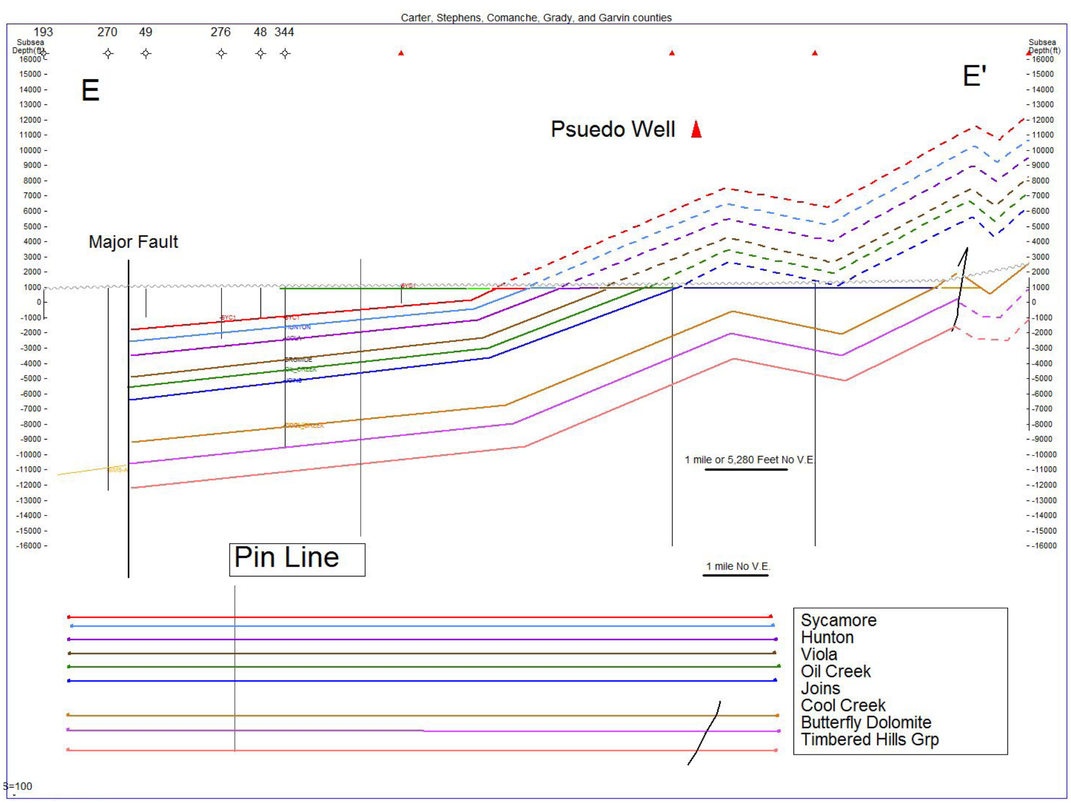

Figure 9: Cross section E-E' through the Tatums Field. The wells used are shown by the number above the well symbol, and can be found in the appendix. Dashed lines represent interpolated layers where erosion has occurred. The Joins Faults is a single segment in E-E'. A major bounding fault was mapped in E-E' due to a deep well that does not penetrate any Mississippian strata. The balanced section is shown below with the pin line. A scale is shown for both the deformed and the balanced section.

ing the Arbuckle Uplift from Sho-Vel-Tum is observed in cross section E-E'. Near the southwest edge of cross section E-E', a well over 3,960 m (13,000 ft) deep does not penetrate any Mississippian strata, however, Mississippian limestone crops out at the surface 6.5 kkm (4 mi) to the northeast. This major fault was also observed in seismic data as a nearly vertical fault with steeply southwest-dipping beds on the Arbuckle side and nearly horizontal beds to the southwest on Sho-Vel-Tum side. This fault was also detected in dip-vector maps by noticeably larger dip vectors along the northeast Tatums Field. In summary, cross sections D-D' and E-E' reveal transpressional faulting on the Arbuckle Uplift as well as a major bounding fault between the Arbuckle Uplift and Sho-Vel-Tum.

The stereonet analyses helps to identify tightness, curvature, and symmetry of the folds in each field as well as the trend and plunge. Folds in Tatums and Sholem Fields are open and symmetrical, as represented by a cluster of poles in the center of the net due to shallow-dipping beds in these two fields. The fold in the Velma Field is relatively open, rounded, and slightly asymmetrical with steeper dip angles along the southwest limb of the anticline. The trend and plunge of the folds are 281°, 3°, in the Tatums Field, 327°, 1.6° in the Sholem Field, and 314°, 1.5° in the Velma Field (Figure 10).

Strain, based on the balanced cross sections, was determined for each field. The ellipse was calculated using the greatest amount of shortening for each field, which is 10% for the Tatums Field, 2% for the Sholem Field, and 31% for the Velma Field. The ellipses show that the shortening precludes any type of flattening strain or associated flexural-flow folding (Behzadi and Dubey, 1980). The distinguishing feature of flexural-slip folding is that bed layers maintain their thickness, whereas in flexural-flow folds they do not (Donath and Parker, 1964). The evidence for flexural-slip folding in the strain ellipses validates the method employed for balancing the cross sections (Figure 11)

Discussion

This project examined changes in deformation intensity and the potential application of balancing techniques to compare the Arbuckle Uplift to Sho-Vel-Tum. Results from the dip-vector maps, balanced cross sections, stereonets, and strain analyses show that shortening increases toward the southwest in Sho-Vel-Tum, but is not a continuation from the Arbuckle Uplift. A major bounding fault observed in seismic data and dip-vector maps is seen in cross section E-E'. This major fault strikes northwest-southeast and sep-

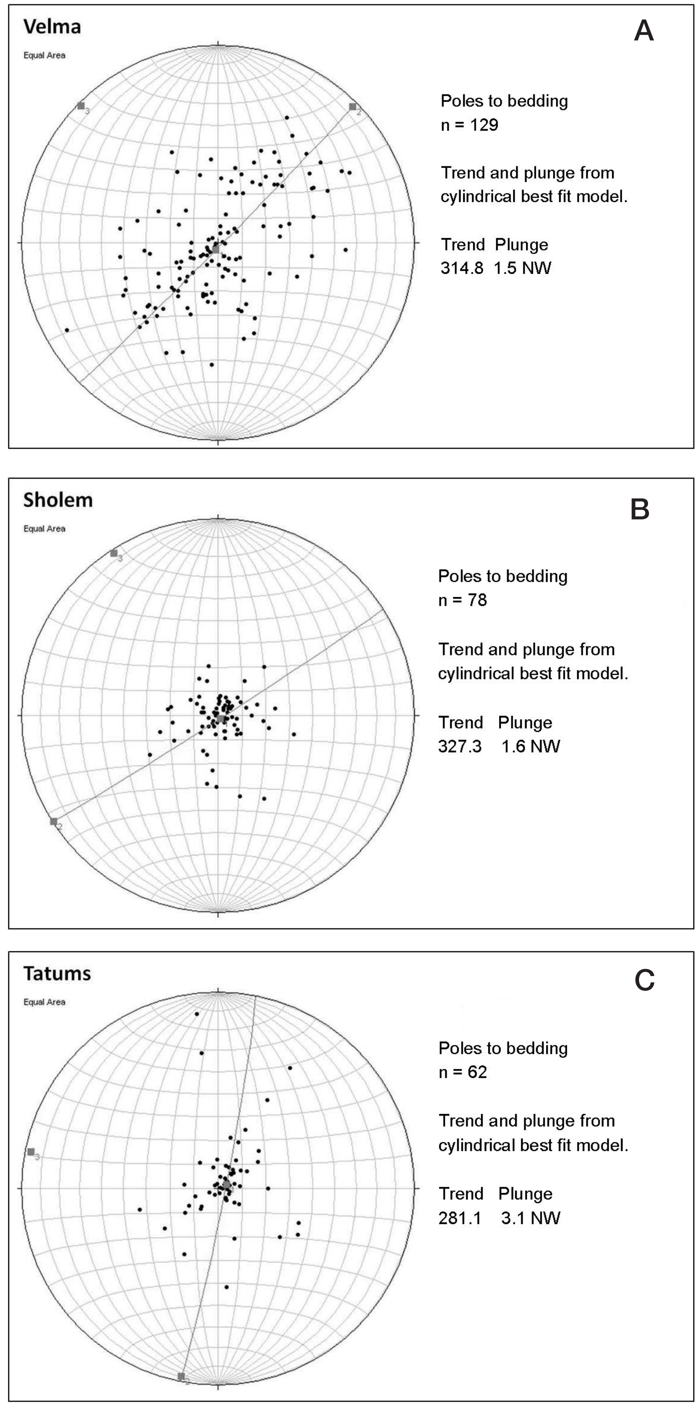

Figure 10. Stereonet analysis of poles to bedding in (A) Velma, (B) Sholem and (C) Tatums Fields.

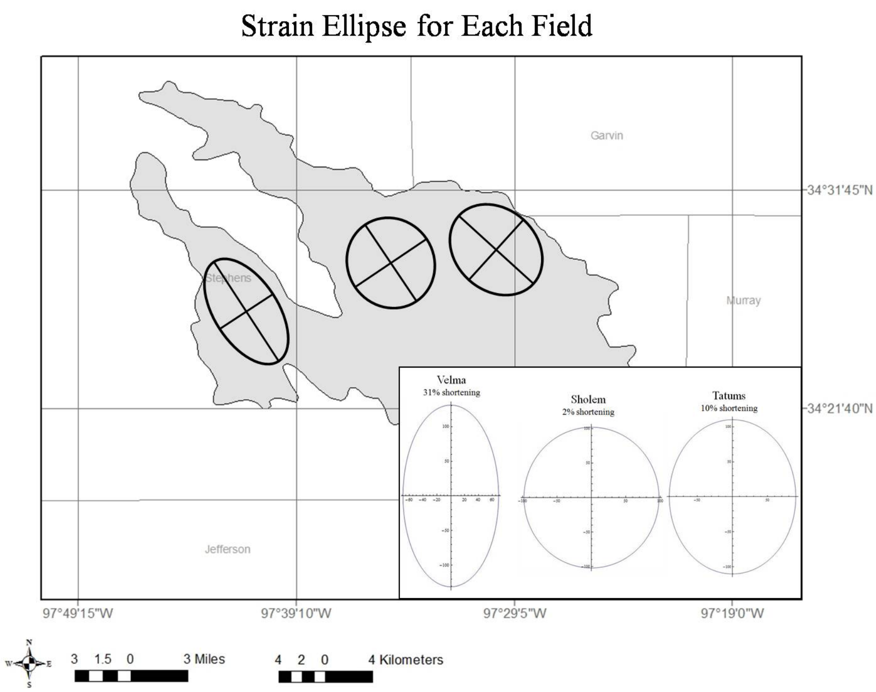

Figure 11. Strain data for Velma, Tatums and Sholem Fields. The strain ellipses show the degree of shortening in each of the cross sections for the fields.

arates the Arbuckle Uplift from Sho-Vel-Tum. Southwest of this fault there is little deformation in the Tatums and Sholem Fields, but deformation increases rapidly in the Velma Field. The balanced cross sections through Sho-Vel-Tum show intense deformation in the Velma Field. The results suggest Sho-Vel-Tum is disconnected structurally from the Arbuckle Uplift.

Although Sho-Vel-Tum is disconnected from the Arbuckle Uplift, the structural styles within each are similar. Both systems are characterized by large, flexural-slip folds that are fault-bounded on the northeast quadrant of the folds. The bounding fault (fault 4) that cuts the main anticline in the Velma Field also trends northwest-southeast and shows a decrease in accommodation room toward the northwest. Cross section A-A' has a greater amount of shortening than cross section B-B' and extends further to the northwest over the major anticline in the Velma Field. The displacements from each backthrust fault extending off of the bounding fault contributes to a greater amount of shortening on cross section A-A' and suggests accommodation room is decreasing toward the northwest along the Velma Anticline, similar to what was observed along the Arbuckle Anticline. We interpret the structural style as transpressional. Fault displacements increase to the northwest suggesting that accommodation room decreases toward the northwest along the anticlinal trend.

The strain ellipses through Sho-Vel-Tum also show that the shortening precludes any type of flattening strain and associated flexural-flow folding. The Arbuckle Anticline and the Velma Anticline both resulted from flexural-slip folding mechanisms as shortening increased during transpression.

Deformation in the Arbuckle Uplift and in Sho-Vel-Tum is partitioned along bounding faults. The fault in northeast Tatums Field is the first bounding fault in Sho-Vel-Tum and separates the highly deformed western Arbuckle Uplift from the lesser deformed Tatums Field. Other bounding faults in Sho-Vel-Tum occur within the Velma Field. The bounding faults extending through Sho-Vel-Tum imitate larger bounding faults extending through the Arbuckle Uplift resulting in similar folding mechanisms and fault trends in each system.

Conclusions

Over 300 well logs were studied and over 500 strike and dip values were calculated using the classic three-point-problem construct. The strike and dip values were used to create a series of dip-vector maps. Five balanced cross sections were constructed connecting the western part of the Arbuckle Uplift to the southwest into Sho-Vel-Tum. The main conclusions that can be drawn from this work are:

1) The structural evolution of Sho-Vel-Tum is similar to but not a continuation of deformation from the Arbuckle Uplift.
2) The trend of folds and faults between the two systems is similar.
3) The fault displacement along anticlines in Sho-Vel-Tum increases to the northwest suggesting accommodation room is decreasing to the northwest along the axis of each anticline.
4) Flexural-slip folding is the dominant mechanism of fold development with accompanying into-the-hinge thrusting.
5) The most reasonable interpretation of Sho-Vel-Tum structure is that of the formation of pop-up features formed in transpression.

REFERENCES CITED

Behzadi, H., and Dubey, A.K., 1980, Variation of interlayer slip in space and time during flexural slip folding: Journal of Structural Geology, v. 2, p. 453-457.

Billingsley, H.R., 1956, Sholom Alechem Oil Field, Stephens and Carter Counties, Oklahoma, *in* Petroleum Geology of Southern Oklahoma, a Symposium: Ardmore Geological Society, v. 1, p. 294-310.

Boyd, D.T., 2002, Map of Oklahoma Oil and Gas Fields: Distinguished by Coalbed Methane and Field Boundaries: Oklahoma Geological Survey Map GM-37, scale 1:500,000.

Brown, W.G., 1984, Washita Valley Fault – A new look at an old fault: Technical Proceedings of the 1981 American Association of Petroleum Geologists Mid-Continent Regional Meeting, p. 68-80.

Carter, D.W., 1979, A study of the strike-slip movement along the Washita Valley Fault, Arbuckle Mountains, Oklahoma: Shale Shaker, v. 30, p. 79-109.

Cederstrand, J.R., 1996, Digital Geologic Map of Ardmore-Sherman Quadrangles, South-Central Oklahoma. U.S. Geological Survey Open-File Report 96-370.

Decker, S., 2002, The Velma and Milroy structures, Ardmore Basin southern Oklahoma (abstract): American Association of Petroleum Geologists Hedberg Conference, Late Paleozoic Tectonics and Hydrocarbon Systems of Western North America – the Greater Ancestral Rocky Mountains Conference, American Association of Petroleum Geologists Search and Discovery Article #90012.

Donath, F.A., and Parker, R.B., 1964, Folds and folding: Geological Society of American Bulletin, v. 75, p. 45-62.

Dott, R.H., 1933, Presidential address: Structural history of the Arbuckle Mountains: Tulsa Geological Society Digest, v. 1, p. 37-40.

Feinstein, S., 1981, Subsidence and thermal history of Southern Oklahoma Aulacogen: Implications for petroleum exploration: American Association of Petroleum Geologists Bulletin, v. 65, p. 2521-2533.

Ferebee, C.D., 1991, Subsidence and basin development in the Southern Oklahoma Aulacogen [M.S. thesis]: Tulsa, Oklahoma, University of Tulsa, 121p.

Granath, J.W., 1989, Structural evolution of the Ardmore Basin, Oklahoma: Progressive deformation in the foreland of the Ouachita collision: Tectonics, v. 8, p. 1015-1036.

Groshong, R.H., Jr., 2006, 3-D Structural Geology: A Practical Guide to Quantitative Surface and Subsurface Map Interpretation, 2nd edition: New York, Springer, 400p.

Ham, W.E., 1951, Structural geology of the southern Arbuckle Mountains: Tulsa Geological Society Digest, v. 19, p. 68-71.

Harmon, R.E., and Tapp, B., 2001, Small-scale inversion feature on the flanks of the Ardmore Basin: Structural study of the Milroy Field, *in* Johnson, K.S., and Merriam, D.F., eds., Petroleum Systems of Sedimentary Basins in the Southern Midcontinent, 2000 Symposium: Oklahoma Geological Survey Circular 106, p. 187-190.

Hoard, J.L., 1956, Tussy sector of the Tatums Field, Carter and Garvin Counties, Oklahoma *in* Petroleum Geology of Southern Oklahoma, a Symposium: Ardmore Geological Society, v. 1, p. 186-206.

Hoffman, P., Dewey, J.F., and Burke, K., 1974, Aulacogens and their genetic relation to geosynclines, with a Proterozoic example from Great Slave Lake, Canada: Society of Economic Paleontologists and Mineralogists Special Publication No. 19, p. 38-55.

Houseknecht, D.W., 1983, Tectonic-sedimentary evolution of the Arkoma Basin: Society of Economic Paleontologists and Mineralogists, Mid-Continent Section, v. 1, p. 3-33.

Jacobson, M.I., 1984, The Harrisburg Trough, Stephens County, Oklahoma: An update, *in* Borer, J.G. II, ed., Technical Proceedings of the 1981 American Association of Petroleum Geologists Mid-Continent Regional Meeting, Oklahoma City Geological Society, p. 127-137.

Johnson, K.S., reviser, 1990, Geologic Map and Sections of the Arbuckle Mountains, Oklahoma: Oklahoma Geological Survey Map GM-31, scale 1:100 000, 1 sheet.

Mitra, S., 1992, Balanced structural interpretations in fold and thrust belts, *in* Mitra, S., and Fisher, G.W., eds., Structural Geology of Fold and Thrust Belts: Baltimore, Johns Hopkins University Press, p. 53-77.

Mount, V.S., Suppe, J., and Hook, S.C. 1990, A forward modeling strategy for balancing cross sections: American Association of Petroleum Geologists Bulletin, v. 74, p. 521-531.

Naruk, S.J., 1989, Geometric analysis and balanced cross-sections of the Arbuckle Mountains and Washita Valley Fault: Shale Shaker, v. 45, p. 10-15.

Perry, W.J., 1988, Tectonic Evolution of the Anadarko Basin Region, Oklahoma: U.S. Geological Survey Bulletin 1989, p. A1-A19.

Rutledge, R.B., 1956, The Velma Oil Field, Stephens County, Oklahoma, *in* Petroleum Geology of Southern Oklahoma, a symposium: Ardmore Geological Society, v. 1, p. 260-281.

Simpson-Carpenter, M.J., 2011, A structural analysis of the Sho-Vel-Tum Field and correlation to the Arbuckle Mountains using balanced cross sections, Stephens and Carter Counties [M.S. thesis]: Tulsa, Oklahoma, University of Tulsa, 117p.

Taff, J.A., 1904, Preliminary Report on the Geology of the Arbuckle and Wichita Mountains in Indian Territory and Oklahoma: U.S. Geological Survey Professional Paper 31, 97p.

Tanner, W.F., 1963, Tectonic patterns in the Appalachian-Ouachita-Oklahoma Mountain complex: Shale Shaker, v. 14, no. 3, p. 2-6.

Tapp, B., 1995, Inversion model for the structural style of the Arbuckle Region, *in* Johnson, K.S., ed., Structural Styles in the Southern Midcontinent, 1992 Symposium: Oklahoma Geological Survey Circular 97, p. 113-118.

Tomlinson, C.W., and McBee, W., 1987, Pennsylvanian sediments and orogenies of Ardmore District, Oklahoma, *in* Rascoe, B., Jr., and Hyne, N.J., eds., Petroleum geology of the mid-continent: Tulsa Geological Society Special Publication No. 3, p. 85-89.

TABLE 1: API NUMBER, WELL, TD AND SPUD DATE FOR WELLS USED IN CROSS SECTION A-A'

Cross section	# Listed	API Number	Well Name	Well No.	TD (ft)	Spud Date
A	541	35137241420000	DOUTHIT	1	7189	07/05/1985
A	542	35137242350000	LUCILLE `A`	1	8550	12/17/1985
A	553	35137245870000	STODDARD B	1	10255	11/05/1987
A	605	35137301020000	HARMON JESSE	1	9012	04/02/1965
A	607	35137301480000	BURKHART A	1	5796	06/11/1965
A	613	35137003390000	PASCHALL	2	7329	05/09/1946
A	642	35137600160000	WESTHEIMER	1	9855	09/18/1955
A	658	35137019320000	COWAN	1	9604	04/17/1955
A	771	35137200600000	M G BURKHART	2	4720	06/02/1966
A	953	35137210440000	VELMA DEEP	1	14493	08/19/1974
A	1010	35137037450000	SCHOOL LAND	1	7346	08/08/1948
A	1044	35137040060000	HARMON-/C/	1	6745	07/12/1957
A	1046	35137040690000	HOLDER	1	7469	06/10/1963
A	1054	35137218320000	VELMA ARBUCKLE UNIT	1	17507	05/16/1978

TABLE 2: API NUMBER, WELL, TD AND SPUD DATE FOR WELLS USED IN CROSS SECTION B-B'.

Cross section	# Listed	API Number	Well Name	Well No.	TD (ft)	Spud Date
B	501	35137059020000	LULA HARRIS	6	7030	01/30/1955
B	547	35137243670000	DAUBE PARTNERSHIP	2-4	7207	07/12/1986
B	659	35137019480000	GATES-GILMORE	1	4800	01/01/1943
B	775	35137203640000	DAUBE	1	10528	08/28/1968
B	819	35137030780000	A M GILMORE	4	7883	01/08/1949
B	820	35137030810000	FRENSLEY-HANSON	1	6816	03/18/1951
B	826	35137030940000	SIDNEY	6	7650	05/08/1950
B	830	35137031090000	ALMA BINDER	1	6860	10/23/1948
B	1078	35137041600000	ROBBERSON /A/	1	5300	08/02/1951
B	1082	35137042110000	DOAK ZIGLER	8	6096	06/29/1954
B	1086	35137042220000	ROBBERSON	6	8556	06/16/1948
B	1090	35137042490000	KUENKEL	1	9110	05/25/1945
B	1091	35137042700000	MARTIN	1-D	8254	01/21/1945
B	1099	35137045350000	FRENSLEY /N/	2	6207	05/17/1952
B	1108	35137224440000	STIEFEL /B/	1-X	10644	08/18/1980
B	1117	35137227970000	MCFARLAND	1	5322	05/26/1981

TABLE 3: API NUMBER, WELL, TD AND SPUD DATE FOR WELLS USED IN CROSS SECTION C-C'.

Cross section	# Listed	API Number	Well Name	Well No.	TD (ft)	Spud Date
C	140	35019031560000	CLEALAND PRUITT	1	7400	02/26/1964
C	143	35019031690000	PECK	6	7321	08/20/1963
C	231	35019213690000	PECK	1	8650	02/15/1975
C	235	35019215750000	JOSIE	1	6518	03/20/1976
C	284	35019211720000	SANNER	1	8050	04/07/1973
C	288	35019212350000	J J HARDIN /A/	1	8423	01/23/1974
C	629	35137005560000	L C RUE	1	6509	03/09/1947
C	635	35137006130000	BOYLES	1	11507	12/03/1951
C	651	35137002290000	DARITY	1	5005	08/16/1947
C	743	35137027490000	MURCHISON	8	6062	09/23/1953
C	786	35137207070000	JOE	1	7300	09/26/1971
C	787	35137207490000	MOBIL	1	13252	01/01/1972
C	809	35137030270000	JAMES HYND	1	5649	04/19/1954
C	893	35137208050000	MYRTLE GREEN	22	7300	09/02/1972
C	975	35137213590000	CORNELIUS /B/	1-14	6300	06/19/1976

TABLE 4: API NUMBER, WELL, TD AND SPUD DATE FOR WELLS USED IN CROSS SECTION D-D'.

Cross section	# Listed	API Number	Well Name	Well No.	TD (ft)	Spud Date
D	14	35019009490000	HIGGINS	1	4944	09/28/1959
D	241	35019220280000	TOLBERT	10-1	5690	04/12/1980
D	244	35019222190000	TOLBERT	3-1	4040	12/21/1980

TABLE 5: API NUMBER, WELL, TD AND SPUD DATE FOR WELLS USED IN CROSS SECTION E-E'.

Cross section	# Listed	API Number	Well Name	Well No.	TD (ft)	Spud Date
E	48	35019038240000	ZELLA LINDSAY	1	2002	06/06/1952
E	49	35019038250000	R J JOHNSON	1	1830	03/16/1961
E	193	35019046370000	H L KNIGHT ESTATE	1	2010	10/02/1960
E	270	35019205800000	JOHNSON	1-31	13293	08/17/1969
E	276	35019210010000	R J JOHNSTON	1	3315	02/04/1972
E	344	35019233870000	SPEAKE	1-29	10500	09/04/1986